

Electrochemical and Theoretical Study of Pyrazole 4-(4,5-dihydro-1H-pyrazol-5-yl)-N,N-dimethylaniline (D) as a Corrosion Inhibitor for Mild Steel in 1 M HCl

R. Chadli,^{a,*} M. Elazouzi,^b I. Khelladi,^c A.M. Elhourri,^c H. Elmsellem,^b
A. Aouniti,^b J. Kajima Mulengi,^a B. Hammouti^b

^a *Laboratoire de chimie organique, substances naturelles et analyses (COSNA),
University of Tlemcen, Algeria*

^b *Laboratoire de chimie appliquée et environnement (LCAE-URAC18), Faculty of sciences,
Oujda, Maroc*

^c *Laboratoire de microscopie, microanalyse de la matière et spectroscopie moléculaire, Dept of
chemistry, Faculty of exact sciences. University Djilali Liabes Sidi Bel Abbes, Algeria*

Received June 28, 2016; accepted December 22, 2016

Abstract

This work is devoted to examine the effectiveness of pyrazoles 4-(4,5-dihydro-1H-pyrazol-5-yl)-N,N-dimethylaniline (D) on corrosion of mild steel in a 1 M HCl solution, using weight loss measurement at concentration effects. The inhibitor (D) was synthesized in our laboratory. The formation of this pyrazole was carried out with hydrazine and α -unsaturated aldehydes, and the structure was checked by spectroscopic means, such as FT-IR, ¹H NMR and ¹³C NMR. Polarization curves and electrochemical impedance spectroscopy (EIS) methods were used to assess both the corrosion rate and inhibition efficiency. Potentiodynamic polarization showed that D behaved as a mixed-type inhibitor. The Nyquist plots showed that, while D concentrations increased, charge-transfer resistance increased and double-layer capacitance decreased, involving increased inhibition efficiency. Adsorption of the inhibitor molecules corresponds to Langmuir adsorption isotherm. Quantum chemical calculations showed that the inhibitor was prone to be protonated in the acid, and the results were in full agreement with experimental observations.

Keywords: Pyrazole; hydrazine; NMR; mild steel; corrosion inhibition; weight loss; electrochemical, DFT method.

Introduction

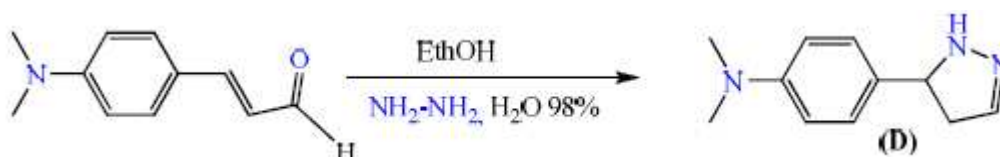
The use of iron and its alloys in daily life is almost found in everyday aspect of life. Iron is used in large amounts in industry, as well as in domestic needs. Iron gained this place by its physicochemical properties, as it is strong, has a high

* Corresponding author. E-mail address: mailchadli@yahoo.fr

density, high melting point and is reliable for life. Despite all these beneficial features, iron is very corrosive, especially in water and air. This corrosion can cause serious damage to the metal, thereby limiting its applications [1–7]. To prevent iron from acidic aggression, the use of organic inhibitors is one of the most practical methods and cost-effective choices to protect metals against corrosion; most of the well-known acid inhibitors are organic compounds containing nitrogen, sulphur and oxygen atoms [8-15]. These organic inhibitors are usually adsorbed on the metal surface via formation of a coordinate covalent bond (chemical adsorption) or electrostatic interaction between the metal and inhibitor (physical adsorption) [16]. This adsorption produces a uniform film, which isolates the metal surface from the aggressive medium, and consequently reduces the extension of corrosion [17].

In this work we were mainly interested in the *N*-heterocyclic inhibitors of iron corrosion in an acidic medium; these *N*-heterocycles of interest are pyrazoles. Pyrazoles derivatives are a very important class of iron corrosion inhibitors [18-28]. As a matter of fact, nitrogen containing heterocycles can be easily protonated in acidic medium, thus exhibiting good inhibitory action on the corrosion of metals in acid solutions. The present study aimed at testing a new compound, namely D, 4-(4,5-dihydro-1H-pyrazol-5-yl)-*N,N*-dimethylaniline, on the corrosion of stainless steel in 1 M hydrochloric acid solution. The study has been performed with various concentrations of D, using potentiodynamic polarization and EIS techniques. Compound D afforded a good anticorrosive activity of steel in 1 M HCl solution, with a 97% efficacy that was reached with the use of 10^{-3} M of D at 25 °C. In order to understand the inhibition of corrosion of mild steel in acidic medium, D chemical quantum parameters were examined and calculated using the density functional theory (DFT) method.

The heterocycle inhibitor was synthesized in ethanol reacting hydrazine and an α,β -unsaturated carbonyl derivative such as 3-(4-(dimethylamino)-phenyl)acrylaldehyde. This reaction provided the pyrazole a very high yield (Scheme 1). This reaction is considered an analogue of reaction of ketenes and aldehydes hydrazines and derivatives [29-33]. The target compound was analysed by FT-IR, ^1H NMR and ^{13}C NMR.



Scheme 1. Synthesis of pyrazole.

Experimental

Synthesis and characterization of the inhibitor

All reactions were carried out under dry nitrogen. I.R spectra were performed on a Mattson Genesis II FTIR instrument. NMR spectra were recorded in CDCl₃ on a Bruker 300 MHz instrument using tetramethylsilane (TMS) as an internal

standard. Melting points were determined on an Electrothermal T1A F3.15A-instrument.

Synthesis of 4-(4,5-dihydro-1H-pyrazol-5-yl)-N,N-dimethylaniline D

To a solution of 3-(4-(dimethylamino) phenyl) acrylaldehyde (1 mmol) in ethanol (10 mL), an equimolar 98% hydrazine monohydrate was added in the presence of acetic acid. The mixture was maintained under reflux for 2 h, until TLC indicated the end of reaction. Then, the reaction mixture was poured in cold water, and the precipitate formed was filtered off, washed and recrystallized in ethanol.

Yield: 76%; mp=142–144°C; IR (KBr, λ_{\max}): 3159, 3066, 2933, 1649, 1531, 1597 cm^{-1} , $^1\text{H NMR}$ (CDCl_3) δ : 2.95 (t, 2H, CH_2), 3.08 (s, 6H, CH_3), 3.17 (t, 1H, CH), 7.17–7.54 (m, 4H, ArH), 8.44 (t, 1H, CH), 9.82 (s, 1H, NH) ppm (Fig. 1); $^{13}\text{CNMR}$ (CDCl_3): δ 40.24, 111.73, 112.01, 123.64, 129.84, 151.76, 162.39 ppm.

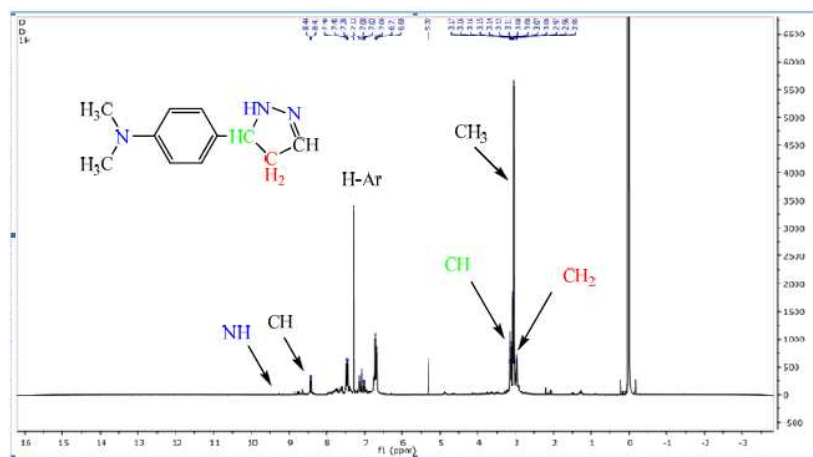


Figure 1. $^1\text{H NMR}$ spectra of (D).

Metal specimens

Steel samples (0.21% C, 0.38% Si, 0.09% P, 0.01% Al, 0.05% Mn and 0.05% S) are used.

Test solution

The aggressive solution 1 M HCl was prepared by the dilution of commercial analytical grade 37% HCl with bi-distilled water. Prior to all measurements, steel samples were polished with different sand paper up to 1200 grade, washed thoroughly with bi-distilled water and dried after washing with acetone. The concentration range of green inhibitor ranged within 10^{-3} and 10^{-6} M.

Methods

Mild steel corrosion behaviour in 1 M HCl was investigated in the absence and presence of D with the help of gravimetical and electrochemical techniques. It was observed that mild steel dissolution rate was very high in 1 M HCl alone, but presence of the inhibitor significantly decreased the corrosion rate of mild steel.

Gravimetric measurements

Coupons for weight loss measurements were cut into $1.5 \times 1.5 \times 0.05$ cm dimensions with the following composition: 0.09% P, 0.01% Al, 0.38% Si, 0.05% Mn, 0.21% C, 0.05% S and Fe. Prior to all measurements, the exposed area was mechanically abraded with 180, 400, 800, 1000 and 1200 grades of emery papers. The specimens were thoroughly washed with bi-distilled water, defatted, and finally washed with ethanol and dried. Gravimetric measurements were carried out in a double walled glass cell equipped with a thermostated cooling condenser. The solution volume was 100 cm³ standard. The immersion time for the weight loss was 6 h at 25 ± 1 °C. In order to get good reproducibility, experiments were carried out in duplicate, and the value given was an average of individual measures. The corrosion rate (v) was calculated using the following equation:

$$v = \frac{W}{S \cdot t} \quad (1)$$

where W is the average weight loss, S the total area, and t the immersion time. With the corrosion rate calculated, the inhibition efficiency E_w was determined as follows:

$$E_w \% = \frac{V_0 - V}{V_0} \cdot 100 \quad (2)$$

V_0 and V are the values of corrosion rate without and with inhibitor, respectively.

Electrochemical measurements

The electrochemical study was carried out using a potentiostat PGZ100 piloted by Voltmaster software. This potentiostat was connected to a cell with three electrode-thermostat with double wall. A saturated calomel electrode (SCE) and platinum electrode were used as reference and auxiliary electrodes, respectively. Anodic and cathodic potentiodynamic polarization curves were plotted at a polarization scan rate of 0.5 mV/s. Before all experiments, the potential was stabilized at free potential during 30 min. The polarization curves were obtained from -800 mV to -200 mV at 308 K. The solution to be analysed was then degassed by bubbling nitrogen. Inhibition efficiency $E_p\%$ was defined as shown in equation (3), where I_{corr} and $I_{\text{corr}(\text{inh})}$ represent corrosion current density values without and with inhibitor, respectively:

$$E_p \% = \frac{I_{\text{corr}} - I_{\text{corr}(\text{inh})}}{I_{\text{corr}}} \cdot 100 \quad (3)$$

The electrochemical impedance spectroscopy (EIS) measurements were carried out with the electrochemical system, which included a digital potentiostat model Voltalab PGZ100 computer at E_{corr} , after immersion in solution without bubbling. After determination of the steady-state current at corrosion potential, sinus wave voltage (10 mV) peak to peak, at frequencies between 100 kHz and

10 mHz, was superimposed on the rest potential. Computer programs automatically controlled the measurements performed at rest potentials after 0.5 hour of exposure at 308 K. The impedance diagrams are given in the Nyquist representation. Inhibition efficiency $E_R\%$ was estimated using the relation (4), where R_t and $R_{t(inh)}$ are the charge transfer resistance values in the absence and presence of inhibitor, respectively.

$$E_R \% = \frac{R_{t(inh)} - R_t}{R_{t(inh)}} \cdot 100 \quad (4)$$

Quantum chemical calculations

Density functional theory (DFT) has often been used [34, 35] to describe the interaction between the inhibitor molecule and the surface, as well as the properties of these inhibitors concerning their reactivity. The molecular band gap was computed as the first vertical electronic excitation energy from the ground state, using the time-dependent density functional theory (TD-DFT) approach as implemented in Gaussian 03 [25]. For this sake, some molecular descriptors, such as HOMO and LUMO energy values, frontier orbital energy gap (E_{gap}), molecular dipole moment (μ), absolute electronegativity (χ), global hardness (η), softness (σ), and fraction of electrons transferred (ΔN) were calculated using the DFT method, and have been used to understand the properties and activity of the newly prepared compounds, and to help in the explanation of the experimental data obtained for the corrosion process.

According to Koopman's theorem [36], the ionization potential (IE) and electron affinity (EA) of the inhibitors were calculated using the following equations:

$$IE = -E_{HOMO} \quad (5)$$

$$EA = -E_{LUMO} \quad (6)$$

Thus, the values of electronegativity (χ) and chemical hardness (η), according to Pearson, with operational and approximate definitions, could be evaluated using the following relations [37]:

$$\chi = \frac{IE + EA}{2} \Leftrightarrow \chi = -\frac{E_{HOMO} + E_{LUMO}}{2} \quad (7)$$

$$\eta = \frac{IE - EA}{2} \Leftrightarrow \eta = \frac{E_{LUMO} - E_{HOMO}}{2} \quad (8)$$

Global chemical softness (σ), which describes the capacity of an atom or group of atoms to receive electrons [38], was estimated by using the equation:

$$\sigma = \frac{1}{\eta} \Leftrightarrow \sigma = \frac{2}{E_{LUMO} - E_{HOMO}} \quad (9)$$

The number of electrons transferred (ΔN) was calculated from the quantum chemical method using the following equation:

$$\Delta N = \frac{\chi_{Fe} - \chi_{inh}}{2(\eta_{Fe} + \eta_{inh})} \quad (10)$$

where χ_{Fe} and χ_{inh} denote the absolute electronegativity of iron and the inhibitor molecule, respectively, and η_{Fe} and η_{inh} denote the absolute hardness of iron and the inhibitor molecule, respectively. The theoretical value $\chi_{\text{Fe}} \approx 7$ eV was used for iron and $\eta_{\text{Fe}} = 0$ was used, assuming that $\text{IE} = \text{EA}$ for bulk metals [39].

Results and discussion

Gravimetric measurements

The inhibition efficiency values for mild steel in 1 M HCl media at different concentrations of the inhibitor are presented in Table 1. It is obvious that the inhibition efficiency increased with an increase in the inhibitor's concentration. This behaviour can be explained based on strong interaction of the inhibitor molecule with the metal surface, resulting in adsorption [40]. The extent of adsorption increases with the increase in concentration of the inhibitor, leading to increased inhibition efficiency.

Table 1. Corrosion speed $V_{\text{corr (inh)}}$ and the efficacy E_w obtained with different concentrations of D at 308 K by gravimetric measurements.

	C (M)	$V_{\text{corr (inh)}}$ (g/m².h)	E_w (%)
HCl	Blank	9.04	-
D	10^{-3}	0.39	96
	$5 \cdot 10^{-4}$	0.85	93
	10^{-4}	1.51	92
	$5 \cdot 10^{-5}$	1.58	82
	10^{-5}	1.73	80
	$5 \cdot 10^{-6}$	2.32	74

In acidic solutions, the maximum inhibition efficiency was observed at an inhibitor concentration of 10^{-3} M (97%). This result can be explained because organic inhibitors suppress the metal dissolution by forming a protective film adsorbed onto the metal surface, and preserve it from the corrosion medium [41].

Adsorption isotherm

Organic inhibitors exhibit inhibition via adsorption on the solution-metal interface, while the adsorption isotherm can provide the basic information about the interaction between the inhibitor and the metal surface. We tested various adsorption isotherms to fit the experimental data, such as Langmuir, Temkin and Frumkin adsorption isotherms. For D, the plot of C versus (C/θ) provided a straight line with a slope nearly 1, and the linear association coefficient (R^2) was also nearly 1 (Fig. 2), showing that the adsorption of (D) on the carbon steel surface could be well described by Langmuir adsorption isotherm (equation 11). This kind of isotherm involves the single layer adsorption characteristic and there is no interaction between the adsorbed inhibitor molecules and the carbon steel surface.

$$\frac{C}{\theta} = \frac{1}{K} + C \quad (11)$$

where C is the concentration of inhibitor, K the adsorption equilibrium constant, and θ is the surface coverage. The constant of adsorption K_{ads} , is related to the standard free energy of adsorption ΔG°_{ads} , with the following equation (12):

$$\Delta G^\circ_{ads} = -RT \cdot \ln (55,55 \cdot K) \quad (12)$$

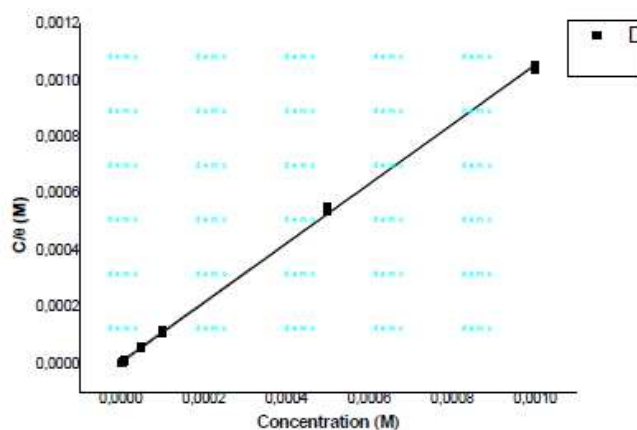


Figure 2. Langmuir adsorption of (D) on the mild steel surface in 1 M HCl solution.

Thermodynamic parameters for the adsorption process were obtained from this figure (Table 2).

Table 2. Thermodynamic parameters for the adsorption of D in 1.0 M HCl on the carbon steel at 25 °C.

	Linear correlation	Slope	K	ΔG° (kJ mol ⁻¹)
D	0.9988	1.046	1,25.10 ⁵	-40,347

The value of ΔG°_{ads} was negative, indicating that the compound investigated was strongly adsorbed on the carbon steel surface, and showing the spontaneity of the adsorption process and stability of the adsorbed layer on the carbon steel surface. Generally, values of ΔG° up to -20 kJ mol⁻¹ are consistent with the electrostatic interaction between the charged molecules and the charged metal (physical adsorption), while those more negative than -40 kJ mol⁻¹ involve sharing or transfer of electrons from the inhibitor molecules onto the metal surface to form a coordinate type of bond (chemisorption) [42]. Therefore, it can be assumed that the adsorption of D on mild steel surface occurs, first due to electrostatic interactions, and then to desorption of water molecules, accompanied by chemical interaction between the adsorbate and metal surface [43].

Polarization measurements

It can be observed that the addition of D caused a remarkable decrease in the corrosion rate, shifting both anodic and cathodic Tafel curves to lower current densities. This indicated that both anodic and cathodic reactions were suppressed, and the suppression became more pronounced with the increase of the concentration of this inhibitor. Electrochemical parameters, such as corrosion

potential (E_{corr}), cathodic Tafel slope (β_c), and corrosion current density (I_{corr}), obtained by extrapolating the Tafel line, are given in Table 3. The corrosion inhibition efficiency ($E_p\%$) of this compound was calculated using the relationship (3). We can classify an inhibitor as cathodic or anodic if the displacement in corrosion potential is more than 85 mV, with respect to corrosion potential of the blank [44]. In the presence of D, the corrosion potential of mild steel shifted only 30 mV to the negative side (vs. SCE). This means that the inhibitor acted as a mixed type inhibitor and showed more pronounced influence in the cathodic polarization plots compared to that in the anodic plots. The parallel cathodic current–potential curves suggested that the addition of this inhibitor did not modify the hydrogen evolution mechanism, and that the hydrogen evolution is activation-controlled. This suppression of the corrosion process may be attributed to the covering of adsorbed pyrazole D molecules on the mild steel surface [45]. For anodic polarization curves of mild steel with this compound, it is clear that the presence of D did not modify the current vs. potential characteristics. The data in Table 3 showed that, when the concentration of the inhibitor increased, the inhibition efficiency also increased and the corrosion current density sharply decreased. This may be due to the adsorption layer of the inhibitor on the metal surface.

Table 3. Potentiodynamic electrochemical parameters of the corrosion of mild steel in 1 M HCl solution with the absence and presence of the investigated inhibitor at 25 °C.

	C (M)	E_{corr} (mV vs. CSE)	I_{corr} (mA/cm ²)	-β_c (mV/dec)	β_a (mV/dec)	E_p (%)
HCl	Blank	-450	2.512	140	185	/
D	10 ⁻³	-422	0.100	66	105	96
	5.10 ⁻⁴	-451	0.160	170	97	93
	10 ⁻⁴	-424	0.184	133	110	92
	5.10 ⁻⁵	-463	0.316	136	70	87
	10 ⁻⁵	-475	0.464	109	85	81
	5.10 ⁻⁶	-467	0.600	84	75	76

Electrochemical impedance spectroscopy

The corrosion of mild steel in 1 M HCl solution in the presence of pyrazole (D) was investigated by EIS at 25 °C after a 30 min exposure. A single semicircle has been observed at high frequency; this could be attributed to charge transfer of the corrosion process and the diameter of the semicircle increased, as the result of increasing inhibitor concentration.

Fig. 3 clearly shows that impedance spectra are not a perfect semicircle. They seem to be depressed in the centre under real axis and look like depressed capacitive loops. Such phenomenon often corresponds to surface heterogeneity that may be the result of surface roughness, dislocations, distribution of the active sites, or adsorption of the inhibitor molecules.

Nyquist plots for mild steel obtained at the interface in the absence and presence of pyrazole (D) at different concentrations are shown in Fig. 4.

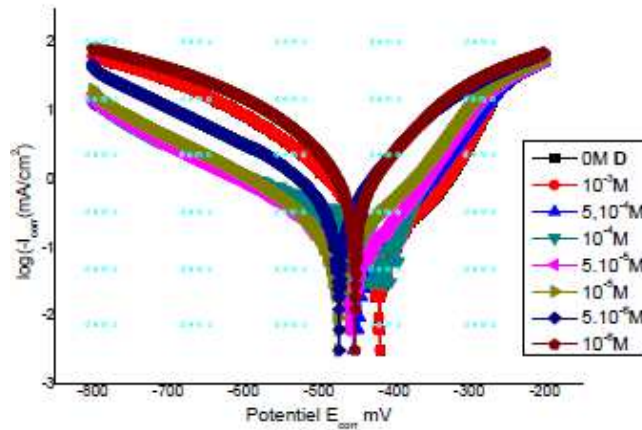


Figure 3. Tafel polarization curves for mild steel in 1 M HCl solution with different concentrations of (D).

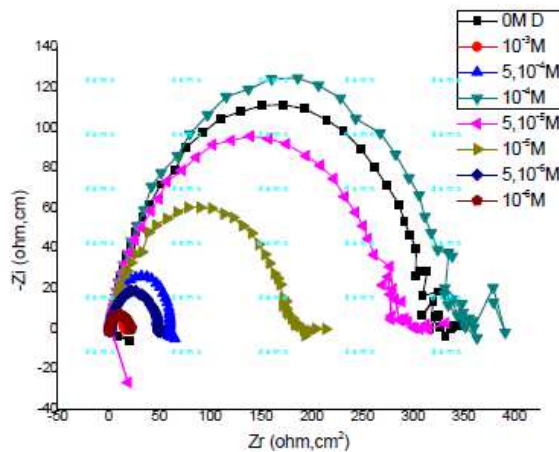


Figure 4. Nyquist plots for mild steel in 1.0 M HCl solution in presence of (D).

An equivalent circuit was introduced to explain the EIS data, as shown in Fig. 5.

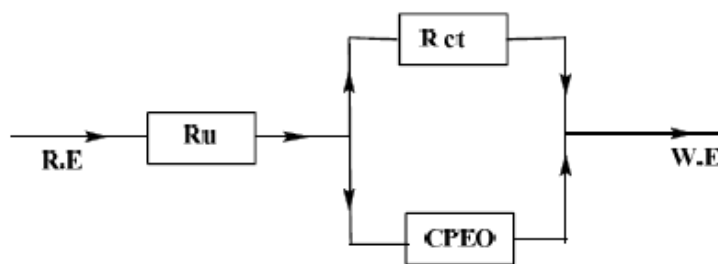
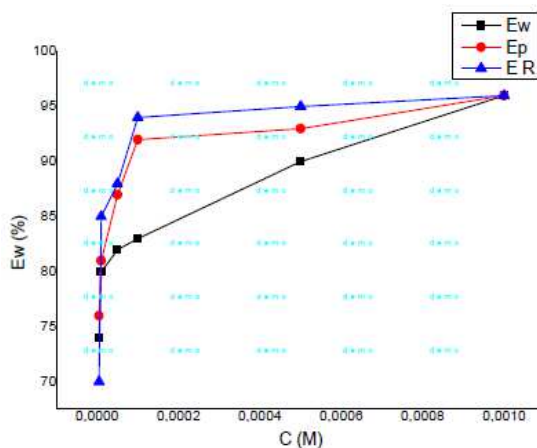


Figure 5. Electrical equivalent circuit model used for the modelling metal/solution.

The inhibition efficiency of the inhibitor $E_R\%$ was calculated from the charge transfer resistance values using equation 4. Table 4 lists impedance parameters of the Nyquist plots of D with different concentrations. The EIS measurement reveals that, at the concentration of 10^{-3} M, the percentage of inhibition efficiency is the highest (97%). The result strongly supports the observation that 10^{-3} M of this compound could work best as an inhibitor.

Table 4. Impedance parameters and inhibition efficiency for mild steel in 1 M HCl solutions, containing different concentrations of (D).

	C (M)	Rs(Ω .cm ²)	Rt (Ω .cm ²)	Cdl (μ F.cm ⁻²)	E_R (%)
HCl	Blank	1.64	14.53	173	/
D	10 ⁻³	1.11	386.5	43.1	96
	5.10 ⁻⁴	1.32	340.2	46.5	95
	10 ⁻⁴	2.32	277	56.5	94
	5.10 ⁻⁵	1.43	121.7	65.3	88
	10 ⁻⁵	1.54	100.8	78.5	85
	5.10 ⁻⁶	1.60	48.25	82.8	70

**Figure 6.** Variation of efficacy with the concentration of the inhibitor D.

The results also show that R_t values increased with the increase in additive concentrations, except for a few cases. The percentage inhibition efficiencies calculated from the R_t values showed that D played the role of a good corrosion inhibitor of mild steel in HCl medium. The CPE values were found to decrease with increase in concentration of the inhibitor solutions (Fig. 6). This behaviour is generally found for systems where inhibition occurred due to the formation of a surface film by the adsorption of the inhibitor on the metal surface [46]. Decrease in CPE, which can result from a decrease in local dielectric constant and/or an increase in the thickness of the electrical double layer, suggested that the inhibitor molecules were absorbed at the metal/solution interface. The values of n obtained for this inhibitor system were close to unity, which shows that the interface behaved in a nearly capacitive way [47].

Quantum chemical calculations

Quantum chemical calculations have been widely used to evaluate the inhibition performance of corrosion inhibitors, which can quantitatively study the relationship between inhibition efficiency and molecular reactivity [48]. By means of this method, the capability of an inhibitor molecule to donate or accept electrons can be predicted with the analysis of global reactivity parameters, such as the energy gap E_{gap} between HOMO and LUMO, chemical hardness η and dipole moment μ .

The higher the value of E_{HOMO} , the greater the ability of the molecule inhibitor to donate electrons, while E_{LUMO} indicates the propensity to accept electrons. By contrast, the lower the E_{LUMO} , the greater the ability of that molecule to accept

electrons. Thus, the binding ability of organics to the metal surface increases with an increase in energy of HOMO and a decrease in the value of energy of LUMO [49]. The energy gap E_{gap} indicates the reactivity tendency of organics toward the metal surface [50]. Thus, E_{gap} has been used to characterize the binding ability of organic compounds to the metal surface [51]. A good corrosion inhibitor behaves as a strong Lewis base, and the electronegativity value of inhibitors is an important parameter in terms of electron transfer between metal and inhibitor. The reactivity of corrosion inhibitors may also be discussed in terms of chemical hardness η , softness σ , parameters molecular dipole moment μ , absolute electronegativity χ [52], and fraction of electrons transferred ΔN [53].

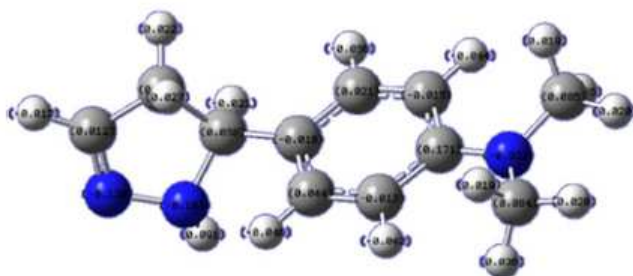


Figure 7. Mulliken charges of D by B3LYP-6-31G (p, d) method.

The adsorption of the inhibitor on the mild steel surface can occur on the basis of donor–acceptor interactions between the lone-pair electron of the heteroatom of the inhibitors and the vacant d orbital of the mild steel surface of Fe atoms.

The optimized geometry, the HOMO and LUMO density distribution of D by B3LYP/6-31G (d, p) method were presented in Fig. 7 and Fig. 8.



Figure 8. HOMO and LUMO frontier molecule orbital density distributions of D.

Table 5. Molecular properties of D from the optimized structure using DFT at the B3LYP/6-31G.

		(D)	(HD) ⁺
E_{HOMO}	(eV)	-5.1614	-14.214
E_{LUMO}	(eV)	-0.0072	-11.275
ΔE_{gap}	(eV)	5.08966	2.93950
μ	(Debye)	3.6051	3,4524
χ	(eV)	2.5843	12.7449
η	(eV)	2.5771	1.46975
σ	(eV ⁻¹)	0.7761	0.58910
ΔN		0.8567	-1.9544

Mulliken charges, according to the numeration of corresponding atoms, are shown in Fig. 7, where it can be observed that both inhibitors had a considerable

excess of negative charge around the nitrogen (-0.322,-0.120, -0.107) and some carbon atoms, indicating that these are the coordinating sites of the inhibitors. The value of E_{HOMO} in the neutral form is higher than in the protonated form (see Table 5). This means that the electron-donating ability of (D) is greater in the neutral form. The E_{LUMO} is directly related to the electron affinity and characterizes the susceptibility of the molecule towards attack by nucleophiles. The diminution of the value of E_{LUMO} increases the ability of the electron-accepting molecule. Thus, the protonated form of pyrazole D exhibits the lowest E_{HOMO} , making the neutral form the most likely to interact with D molecule. Low values of the energy and gap E_{gap} in the protonated form of D can indicate a good stability of the formed complex (inhibitor-Fe) on the metal surface, therefore improving the corrosion resistance of mild steel in 1 M HCl medium [54]. The high value of the dipole moment of pyrazole in the neutral and protonated forms probably indicates strong dipole–dipole interactions of D molecules and the metallic surface. Finally, and according to Lukovits, if $\Delta N < 3.6$, the inhibition efficiency increased with increasing electron-donating ability at the metal surface [7]. In this study, the value of ΔN for D was less than 3.6 for both neutral and protonated forms. This shows that the increase in inhibition efficiency was solely due to the electron-donating ability of D in both forms.

Inhibition mechanism

From the results obtained from different electrochemical and weight loss measurements, we can conclude that pyrazole D inhibited the corrosion of mild steel in 1 M HCl through its adsorption at the metal/solution interface. D can easily be protonated, because its molecules are made of planer aromatic rings of benzene and the pyrazole ring, and it also contains π electrons. Generally, the inhibition of metallic corrosion in acidic solutions first occurs through electrostatic interaction of protonated molecules with already adsorbed chloride ions; second, through donor–acceptor interactions between the p electrons of the aromatic ring and the vacant d-orbital of the iron atoms; and third, from interactions between unshared electron pairs of hetero atoms and the vacant d-orbital of the iron surface atoms. In this study, the calculated $\Delta G_{\text{ads}}^{\circ}$ value indicates that the adsorption of D on the mild steel surface follows both physisorption (ionic) and chemisorption (molecular) mechanisms.

Conclusions

The results obtained during this investigation lead us to draw the following main points:

- The pyrazole D or 4-(4,5-dihydro-1H-pyrazol-5-yl)-*N,N*-dimethylaniline shows good inhibitive properties for mild steel corrosion in 1.0 M HCl solution.
- The inhibition efficiency increases with an increasing concentration of the inhibitor.
- The results of potentiodynamic polarization measurements demonstrate that D behaves as a mixed type inhibitor and could suppress both anodic metal dissolution and cathodic hydrogen evolution reactions.

- D, on the metal surface, obeyed Langmuir adsorption isotherm. The value of the adsorption equilibrium constant shows that the inhibitor is strongly adsorbed on the metal surface.
- The adsorption of D on the steel surface obeys the statistical physics adsorption model. Furthermore, the obtained values of $\Delta G^{\circ}_{\text{ads}}$ indicate that the adsorption of (D) molecules onto the steel surface is a spontaneous process involving both physisorption and chemisorption mechanisms.
- The quantum mechanical approach may well be able to foretell molecule structures that are better for corrosion inhibition.

Acknowledgments

The authors are indebted to General Directorate for Scientific Research and Technological Development (Ministry of Higher Education and Scientific Research Algeria) and the laboratory of Chemistry and Environment (LCAE-URAC18), Faculty of Sciences, Oujda, Morocco, for financial support of this work.

References

1. Adejoro IA, Ojo FK, Obafemi SK. Corrosion inhibition potentials of ampicillin for mild steel in hydrochloric acid solution. *J Taibah Univ Sci.* 2015;9:196–202.
2. Hmamou DB, Salghi R, Zarrouk A, et al. Weight Loss, Electrochemical, quantum chemical calculation, and molecular dynamics simulation studies on 2-(Benzylthio)-1,4,5-triphenyl-1H-imidazole as an inhibitor for carbon steel corrosion in hydrochloric acid. *Ind Eng Chem Res.* 2013;52:14315–14327.
3. Zarrok H, Saddik R, Oudda H, et al. 5-(2-Chlorobenzyl)-2,6-dimethylpyridazin-3-one: An efficient Inhibitor of C38 steel corrosion in hydrochloric acid. *Der Pharm Chem.* 2011;3:272–282.
4. Ghazoui A, Saddik R, Benchat N, et al. The Role of 3-Amino-2-Phenylimidazo[1,2-a]Pyridine as Corrosion Inhibitor for C38 Steel in 1M HCl. *Der Pharm Chem.* 2012;4:352–364.
5. Al Hamzi AH, Zarrok H, Zarrouk A, et al. The Role of Acridin-9(10H)-one in the Inhibition of Carbon Steel Corrosion: Thermodynamic, Electrochemical and DFT Studies. *Int J Electrochem Sci.* 2013;8:2586–2605.
6. Goulart CM, Esteves-Souza A, Martinez-Huitle CA, et al. Experimental and theoretical evaluation of semicarbazones and thiosemicarbazones as organic corrosion inhibitors. *Corros Sci.* 2013;67:281–291.
7. Aouniti A, Elmsellem H, Tighadouini S, et al. Schiff's base derived from 2-acetyl thiophene as corrosion inhibitor of steel in acidic medium. *J Taibah Univ Sci.* 2015;263:12.
8. Zarrouk A, Hammouti B, Zarrok H, et al. Temperature Effect, Activation Energies and Thermodynamic Adsorption Studies of L-Cysteine Methyl Ester Hydrochloride As Copper Corrosion Inhibitor In Nitric Acid 2M. *Int J Electrochem Sci.* 2011;6:6261–6274.

9. Zarrouk A, Hammouti B, Dafali A, et al. L-Cysteine methyl ester hydrochloride: A new corrosion inhibitor for copper in nitric acid. *Der Pharm Chem*. 2011;3:266–274.
10. Zarrouk A, Hammouti B, Zarrok H, et al. N-containing organic compound As An Effective Corrosion Inhibitor For Copper In 2M HNO₃: Weight Loss and Quantum Chemical Study. *Der Pharm Chem*. 2011;3:263–271.
11. Ghazoui A, Bencat N, Al-Deyab SS, et al. An Investigation of Two Novel Pyridazine Derivatives as Corrosion Inhibitor for C38 Steel in 1.0 M HCl. *Int J Electrochem Sci*. 2013;8:2272–2292.
12. Zarrouk A, Zarrok H, Salghi R, et al. The Adsorption and Corrosion Inhibition of 2-[Bis-(3,5-dimethyl-pyrazol-1-ylmethyl)-amino]-pentanedioic Acid on Carbon Steel Corrosion in 1.0 m HCl. *Int J Electrochem Sci*. 2012;7:10215–10232.
13. Bendaha H, Zarrouk A, Aouniti A, et al. Adsorption and corrosion inhibitive properties of some tripodal pyrazolic compounds on mild steel in hydrochloric acid systems. *Phys Chem News*. 2012;64:95–103.
14. Zarrok H, Zarrouk A, Salghi R, et al. Dimethylquinoxalin-2-(1H)-one for inhibition of acid corrosion of carbon steel. *J Chem Pharm Res*. 2012;4:5048–5055.
15. Zarrok H, Al Mamari K, Zarrouk A, et al. Gravimetric and Electrochemical Evaluation of 1-allyl-1Hindole-2,3-dione of Carbon Steel Corrosion in Hydrochloric Acid. *Int J Electrochem Sci*. 2012;7:10338–10357.
16. Daoud D, Douadi T, Issaadi S, et al. Adsorption and corrosion inhibition of new synthesized thiophene Schiff base on mild steel X52 in HCl and H₂SO₄ solutions. *Corros Sci*. 2014;79:50–58.
17. Avci G. Inhibitor effect of N, N'-methylenediacrylamide on corrosion behavior of mild steel in 0.5 M HCl. *Mater Chem Phys*. 2008;112:234–238.
18. Meresht ES, Farahani TS, Neshati J. 2-Butyne-1, 4-diol as a novel corrosion inhibitor for API X65 steel pipeline in carbonate/bicarbonate solution. *Corros Sci*. 2012;54:36–44.
19. Quraishi MA, Jamal D. Dianils: New and Effective Corrosion Inhibitors for Oil-Well Steel (N-80) and Mild Steel in Boiling Hydrochloric Acid. *Corrosion*. 2000;56:156.
20. Benabdellah M, Yahyi A, Dafali A, et al. Corrosion inhibition of steel in molar HCl by triphenyltin2–thiophene carboxylate. *Arab J Chem*. 2011;4:343.
21. Elayyachy M, Hammouti B, El Idrissi A, et al. Adsorption and corrosion inhibition behavior of C38 steel by one derivative of quinoxaline in 1 M HCl. *Port Electrochim Acta*. 2011;29:57.
22. Sykes JM. Silver Jubilee review 25 years of progress in electrochemical methods. *Br Corros J*. 1990;25:175-183.
23. Chatterjee P, Banerjee MK, Mukherjee JP. Synergistic inhibition of inorganic anions with pyridine-derivatives for steel in hydrochloric-acid. *Indian J Technol*. 1991;29:191.
24. Bockris JM, Yang B. The mechanism of corrosion inhibition of iron in acid solution by acetylenic alcohols. *J Electrochem Soc*. 1991;138:2237.

25. Zarrouk A, Warad I, Hammouti B, et al. The effect of temperature on the corrosion of Cu/HNO₃ in the presence of organic inhibitor: part-2. *Int J Electrochem Sci.* 2010;5:1516.
26. Vermilyea DA. In: *Metal Corrosion*. London: Butterworths; 1962.
27. Bentiss F, Traisnel M, Chaibi N, et al. 2, 5-Bis (n-methoxyphenyl)-1,3,4-oxadiazoles used as corrosion inhibitors in acidic media: correlation between inhibition efficiency and chemical structure. *Corros Sci.* 2002;44:2271.
28. El Ouali I, Hammouti B, Aouniti A, et al. Thermodynamic characterisation of steel corrosion in HCl in the presence of 2-phenylthieno (3, 2-b) quinoxaline. *J Mater Environ Sci.* 2010;1:1.
29. Khaled KF, Abdelshafi NS, El-Maghraby A, et al. Molecular level investigation of the interaction of cerium dioxide layer on steel substrate used in refrigerating systems. *J Mater Environ Sci.* 2011;2:166.
30. Uhrea J, Aramaki K. A Surface-Enhanced Raman Spectroscopy Study on Adsorption of Some Sulfur-Containing Corrosion Inhibitors on Iron in Hydrochloric Acid Solutions. *J Electrochem Soc.* 1991;138:3245.
31. Almirante N, Cerri A, Fedrizzi G, et al. A general, [1+4] approach to the synthesis of 3(5)-substituted pyrazoles from aldehydes. *Tetrahedron Lett.* 1998;39:3287-3290.
32. Grandi R, Messerotti W, Pagnoni UM, et al. Decomposition of conjugated p-tosylhydrazones in base. Partition between solvolysis and cycloaddition products. *J Org Chem.* 1977;42:1352-1355.
33. Aggarwal VK, Vicente J, Bonnert RV. A novel one-pot method for the preparation of pyrazoles by 1, 3-dipolar cycloadditions of diazo compounds generated in situ. *J Org Chem.* 2003;68:5381-5383.
34. Corradi A, Leonelli C, Rizzuti A, et al. New "green" approaches to the synthesis of pyrazole derivatives. *Molecules.* 2007;12:1482-1495.
35. Mohareb RM, El-Sayed NNE, Abdelaziz MA. Uses of cyanoacetylhydrazine in heterocyclic synthesis: novel synthesis of pyrazole derivatives with anti-tumor activities. *Molecules.* 2012;17:8449-8463.
36. Chaudhary RS, Sharma S. The influence of auramine 0 on the corrosive behaviour of mild steel. *Ind J Chem Technol.* 1999;6:202-206.
37. Hmamou DB, Salghi R, Zarrouk A, et al. Investigation of corrosion inhibition of carbon steel in 0.5 M H₂SO₄ by new bipyrazole derivative using experimental and theoretical approaches. *J Environ Chem Eng.* 2015;3:2031-2041.
38. Liu H, Zhu L, Zhao Q. Schiff base compound as a corrosion inhibitor for mild steel in 1 M HCl. *Res Chem Intermed.* 2015;41:4943-4960.
39. El Ouali I, Hammouti B, Aouniti A, et al. Thermodynamic characterisation of steel corrosion in HCl in the presence of 2-phenylthieno (3, 2-b) quinoxaline. *J Mater Environ Sci.* 2010;1:1-8.
40. Khaled KF, Abdelshafi NS, El-Maghraby A, et al. Molecular level investigation of the interaction of cerium dioxide layer on steel substrate used in refrigerating systems. *J Mater Environ Sci.* 2011;2:166-173.

41. Uhrea J, Aramaki K. A Surface-Enhanced Raman Spectroscopy Study on Adsorption of Some Sulfur-Containing Corrosion Inhibitors on Iron in Hydrochloric Acid Solutions. *J Electrochem Soc.* 1991;138:3245.
42. Adejoro IA, Ojo FK, Obafemi SK. Corrosion inhibition potentials of ampicillin for mild steel in hydrochloric acid solution. *J Taibah Univ Sci.* 2015;9:196-202.
43. Gomma GK. Corrosion of low-carbon steel in sulphuric acid solution in presence of pyrazole—halides mixture. *Mater Chem Phys.* 1998;55:241–246.
44. Cheng S, Chen S, Liu T, et al. Carboxymethylchitosan as an ecofriendly inhibitor for mild steel in 1 M HCl. *Mater Lett.* 2007;61:3276–3280.
45. Elmsellem H, Karrouchi K, Aouniti A, et al. Theoretical prediction and experimental study of 5-methyl-1H-pyrazole-3-carbohydrazide as a novel corrosion inhibitor for mild steel in 1.0 M HCl. *Der Pharma Chemica.* 2015;7:237-245.
46. Donahue FM, Nobe K. Theory of organic corrosion inhibitors adsorption and linear free energy relationships. *J Electrochem Soc.* 1965;112:886–891.
47. Mahgoub FM, Abdel-Nabey BA, El-Samadisy YA. Adopting a multipurpose inhibitor to control corrosion of ferrous alloys in cooling water systems. *Mater Chem Phys.* 2010;120:104–108.
48. Fawcett WR, Kovacova Z, Motheo AJ, et al. Application of the ac admittance technique to double-layer studies on polycrystalline gold electrodes. *J Electroanal Chem.* 1992;326:91–103.
49. Rosenfield IL. *Corrosion Inhibitors.* New York: Mc Graw-Hill; 1981.
50. Obi-Egbedi NO, Obot IB, El-Khaiary MI. Quantum chemical investigation and statistical analysis of the relationship between corrosion inhibition efficiency and molecular structure of xanthene and its derivatives on mild steel in sulphuric acid. *J Mol Struct.* 2011;1002:86–96.
51. El-Haddad NM, Elattar KM. Synthesis, characterization and inhibition effect of new antipyrinyl derivatives on mild steel corrosion in acidic solution. *Int J Ind Chem.* 2015;6:105–117.
52. Yadav M, Gope L, Sarkar TK. Synthesized amino acid compounds as eco-friendly corrosion inhibitors for mild steel in hydrochloric acid solution: electrochemical and quantum studies. *Res Chem Intermed.* 2016;42:2641–2660.
53. Elbakri M, Touir R, Touhami MB, et al. Inhibiting effects of benzamide derivatives on the corrosion of mild steel in hydrochloric acid solution. *Res Chem Intermed.* 2013;39:2417–2433.
54. Obot IB, Obi-Egbedi NO, Ebenso EE, et al. Experimental, quantum chemical calculations, and molecular dynamic simulations insight into the corrosion inhibition properties of 2-(6-methylpyridin-2-yl)oxazolo[5,4-f][1,10]phenanthroline on mild steel. *Res Chem Intermed.* 2013;39:1927–1948.